The Effect of Step Change in Surface Roughness on a Channel Flow

Suketsugu NAKANISHI* and Hideo OSAKA**

(Received July 14, 1990)

Abstract

The present paper was concerned with a part of the series of study on the flow in a rough wall channel by authors. For the response of a channel flow to the step change in wall condition, the flow through a two-dimensional channel with short length of rough surface has been investigated numerically. The roughness elements were of the repeated square ribs with the pitch ratio $W/h=2$ (W and h denote the roughness spacing and height, respectively). The length of rough surface was equivalent to the channel width (corresponding to an "impulse" of surface roughness for the turbulent boundary layer). The surfaces of upstream and downstream from roughness were smooth and were of sufficient length to allow a fully developed in the smooth wall channel (plane Poiseuille flow) to be established. The Navier-Strokes equations (stream function-vorticity formulation) were solved by the finite difference method using the pseudo-unsteady technique. The calculation was performed for the flow in the different three cases of rough wall channel, and for the range of the Reynolds number $Re<$ 1000. From the calculation results, the flow pattern over the rough wall, the behavior of vortex in the roughness groove, the velocity distribution, the pressure distribution along the channel and the distribution of wall shear stress were presented. On the first stage, the particular attention was paid to the comparision of flow structure in the rough wall channel for the different three cases. The results showed that the flow structure varied with the different three cases of rough wall chnnel. The distance of readjustment to the plane Poiseuille flow (relaxation distance) depended on both the geometry of rough wall and the Reynolds number. It was noticeable results that the effects of roughness on the flow extended to the upstream region from surface (its distance being roughly 10 times roughness height for the case the upstanding roughness at $Re=100$).

1. Introduction

The laws of friction on the flow over the rough surface are of great practical importance, so the study on them began very early [1] . Apart from the practical requirement of fluids engineering, the flow over the rough surface is also of fundamental interest as for the response of a flow to sudden pertubations (such as the response of the flow to a step change in surface roughness) [2~4]. Furthermore, in recent years, the analysis of the flow over the rough wall in the condition of relatively low velocity region has become very important problem for the fluids engineering and heat-mass transfer. For the case of the flow over the rough wall consisting of repeated square ribs, it is especially interested in the engineering application such as the cooling flow over the electronic devices and the circuit board mounted IC package [5~11]. Such flow is closely related to the flow through a corrugated and a wavy tube with

* Department of Physics, Hiroshima Institute of Technology.
**Department of Mechanical Engineering, Yamaguchi University.

application to medical devices. For example, the corrugated and the wavy tube have been used to the arterial prostheses and in the high-performance mass transfer devices such as an extra-corporeal membrane oxygenator and a kidney dialyser [12~18]. Moreover, in the medical applications, the turbulent flow must be avoided because of the risk of damage to formed elements in blood, so the laminar flow is rather to be used. In spite of the demand from various engineering fields as described above, it can not be declared that the fundamental knowledges and data are sufficiently obtained for the laminar flow over the rough wall. Accordingly, the laminar flow through a two-dimensional rough channel, where the rough wall consists of the repeated and embedded square ribs, has been investigated numerically by authors, and a part of results of this numerical studies have already been reported in the Transaction of JSME and so on [19~25]. In the extensive region of the pitch ratio and the Reynolds number, the detailed calculations have been performed for the cases of the both parameter to be changed systematically. From that calculation results, the relation between the flow structure and the dynamical characteristics, that is, the dynamical characteristic changed with the variation of the flow pattern depending on both the pitch ratio and the Reynolds number, were presented in those reports. For all that the detailed calculations for the flow in the channel with roughness elements embedded from wall surface (hereinafter reffered to as embedded rough wall), those reports have not been discussed for the case of flow in the channel with roughness elements upstanding from wall surface (hereinafter reffered to as upstanding rough wall). The flow in the upstanding rough wall channel is interesting from the fluid dynamical point of view, also with respect to the heat-mass of IC packages (in the most case, the IC packages mounted circuit boards can be treated as the upstanding roughness elements).

In this work, the flow in a two-dimensional channel with short region of rough surface consisting of repeated square ribs has been investigated numerically. The different three cases of rough wall channel are considered as follows; the cases both upper and lower walls being embedded rough surface, of both upper and lower walls being upstanding rough surface, and of only lower wall being upstanding rough surface. The calculation is performed for the range of the Reynolds number $Re<1000$, but for the only case of the pitch ratio $W/h=2$ considering the general situation of electronic circuit boards which are densely mounted with the IC packages. On the first stage, particular attention is paid to the flow structure through the rough wall channel in this paper. From the calculation results as the stream lines, the velocity distribution, the shear stress on the rough wall and the pressure distribution at the center line of channel, the flow structure for the different three cases of rough wall channel is compared with each case. The response of the channel flow to a short length in surface roughness is investigated with presented calculation results. In a brief addition, the effect of roughness geometory for the characteristic of heat transfer is discussed deductively with the flow structure.

2. Basic Equations and Calculation Model

Consider the laminar flow in a two-dimensional channel with roughness elements. The governing equations for the two-dimensional flow of a Newtonian fluid are the

Navier-Stokes equations and the continuity equation. By introducing the vorticity ω(where $\omega=\partial v/\partial x-\partial u/\partial y$) and the stream function ψ(where $u=\partial\psi/\partial y, v=-\partial\psi/\partial x$), one obtain the vorticity transport equation in the well-known form

$$\frac{\partial\omega}{\partial t}=\frac{\partial\psi}{\partial x}\frac{\partial\omega}{\partial y}-\frac{\partial\psi}{\partial y}\frac{\partial\omega}{\partial x}+\frac{1}{Re}\nabla^2\omega \tag{1}$$

$$\omega=-\nabla^2\psi, \tag{2}$$

here, $\nabla^2=\partial^2/\partial x^2+\partial^2/\partial y^2$,

where Re is the Reynolds number, $Re=UH/\nu$, U denotes the mean fluid velocity in the channel, H the width of channel and the kinematic viscosity of the fluid, respectively. Equations (1) and (2) are expressed in the non-dimensional forms using the reference length, velocity and time being H, U and H/U, respectively. Calculation model is the steady laminar flow in the two-dimensional channel with short region of rough surface as shown in Fig.1. The rough surface consists of a series of five square ribs ($h=b$) with spacing w and roughness height h. The roughness height h and the pitch ratio w/h are chosen the constant value of $h/H=0.1$ and $w/h=2$, respectively. Three cases of rough wall channel using this rough surface are considered as follows;

i) the rough surface is embedded in the upper and lower walls of channel on the form of embedded rough wall (to be named as the model I).

ii) the rough surface is attached to the upper and lower walls of channel on the form of upstanding rough wall (to be named as the model II), and

iii) the rough surface is attached to the only lower wall of channel with the condition of the same forms as rough wall of the model II (to be named as the model III).

as shown in Fig.2 (a)~(c). The region of rough surface is settled to the location at the distance L_{in} from the upstream boundary of channel. The distance L_{in} and the channel length L (L being the length of computational region) are decided with the condition of vanishing the influence of rough wall on the flow at the upstream and the downstream boundaries of channel. For each model of rough wall channel described above, the preliminary test calculation in order to obtain the values of L_{in} and L was performed for a few flow cases.

The boundary conditions in the computational region are given as follows;

i) the velocity vanishes on the wall surface by the conditions of non-penetration and non-slip at the wall and

ii) the stream function and the vorticity at the upstream and downstream boundaries are given by the plane Poiseuille flow.

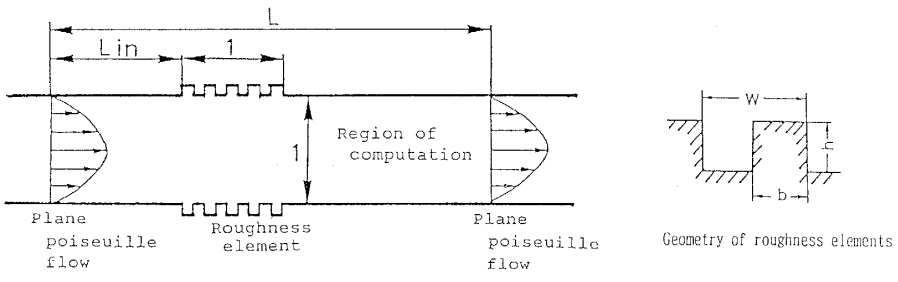

Fig. 1 Calculation model

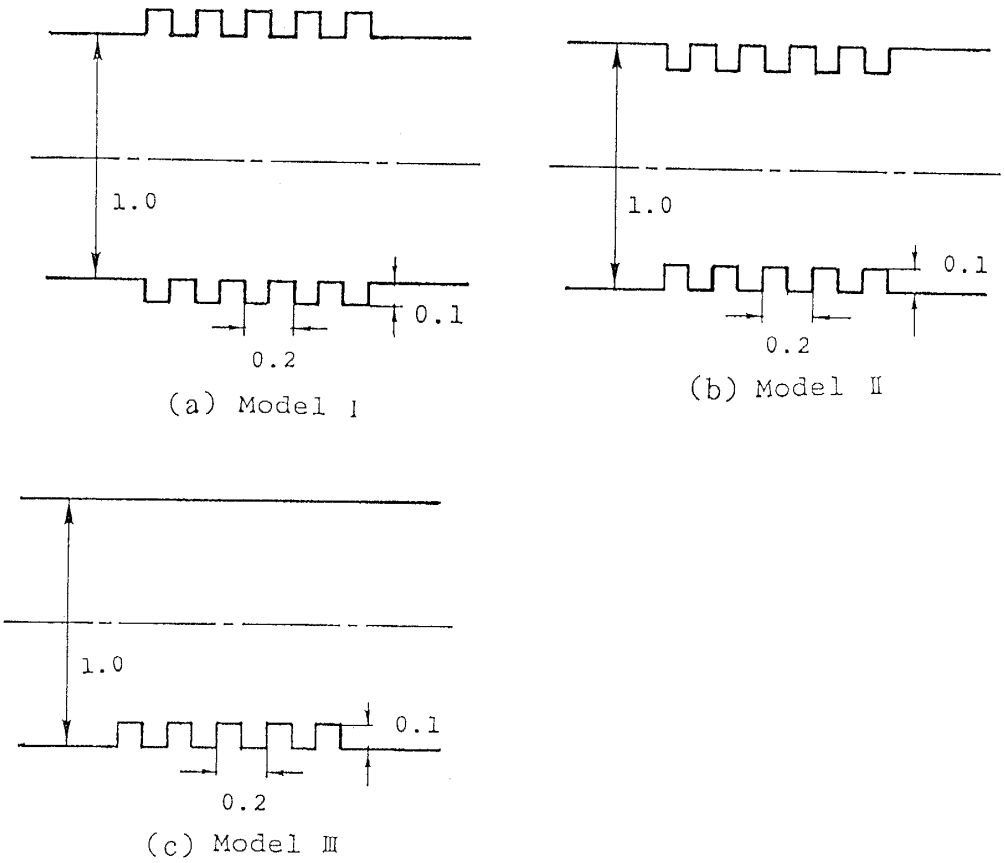

Fig. 2 Rough surface model

The difference equations are derived from the equations (1) and (2) using the forward-time and centered-space differences, and are solved by the pseudo-unsteady method in order to obtain the steady solsution as $t \rightarrow \infty$. The mesh constant is taken as 1/50 throughout the numerical work in this paper. The convergence criterion is defined as $| \psi^{(n+1)}-\psi^{(n)} | \leqq 10^{-5}$, where the superscripts (n) indicate the value at the n-th loop, and $| \omega(t+\Delta t)-\omega(t) | 10 \leqq^{-5}$.

3. Results and Discoussions

3.1 *Flow patterns*

In the order to research on the difference of both flow patterns in the upstanding rough wall channel and the embedded rough wall channel, the flow patterns near region of rough surface are presented by drawing the stream lines. In Fig.3, the flow patterns for the case of model I and model III at the Reynolds number $Re=100$ are shown as an example of the embedded rough wall and the upstanding rough wall channels. As can be seen in Fig.3, the stable separation vortex is formed in the roughness groove for the both cases of model I and model III. For the case model I, gradual development of this vortex is observed as the location of roughness groove being the further downstream from the first roughness groove (upstream end of rough surface). In contrast with this tendency, that of model III shows the decaying tendency,

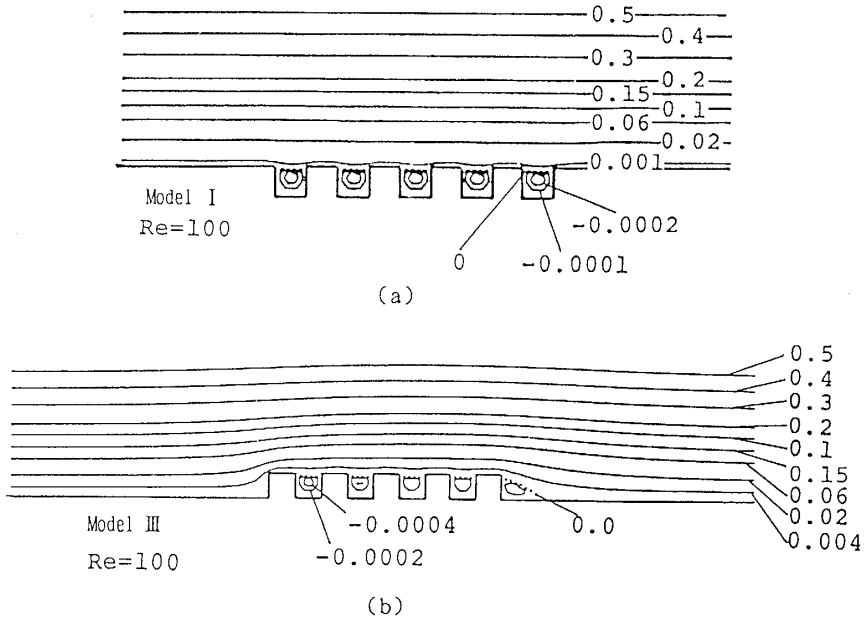

Fig. 3 Stream lines (Re=100); (a) Model I, (b) Model III

that is, the most developed separation vortex in the first roughness groove is observed, and the vortex in the following stage of successive roughness groove is decaying with distance to the downstream direction. As to the different of both tendencies described above, it can be considered that the vortex pattern in the groove depends on the difference in construction of the upstanding and the embedded rough surface. So the vortex pattern in the groove for the case of model II (which is the upstanding rough wall channel) shows the similar tendency qualitativelly as the case of model III, but the stream line of its flow pattern is not presented in this paper.

Turning now the viewpoint from vortex pattern in the groove to the flow pattern over the rough wall, the flow near the wall shows the periodic flow pattern in the similitude of the roughness geometry. For the case of model I, this periodic flow pattern becomes indistinct with increasing the distance from the wall, and eventually parallel at the central region of channel. On the other hand, the flow pattern for the case of model III is affected considerably by the rough surface of lower wall of channel, and its influence reaches the center line of channel as shown in Fig.3(b). Namely, it can be understood that the asymmetric flow pattern with respect to the center line is caused by the effect of asymmetric geometry of rough wall channel (see in Fig.2(c)).

In the next step, the effect of rough surface on the flow pattern is further researched with the distribution of flow velocity. In Fig.4(a)~(c), the streamwise velocity distribution at the constant height from the lower smooth wall of channel is shown for the case of the Reynolds number $Re=100$ of each model I, II, III. As observed stream lines in Fig.3, the velocity distribution near the rough wall also shows the periodic flow distribution and this velocity distribution becomes indistinct with increasing the distance from the wall. In the region of rough surface, the velocity near the wall slightly increases compared with that of smooth wall, and gradually increases with

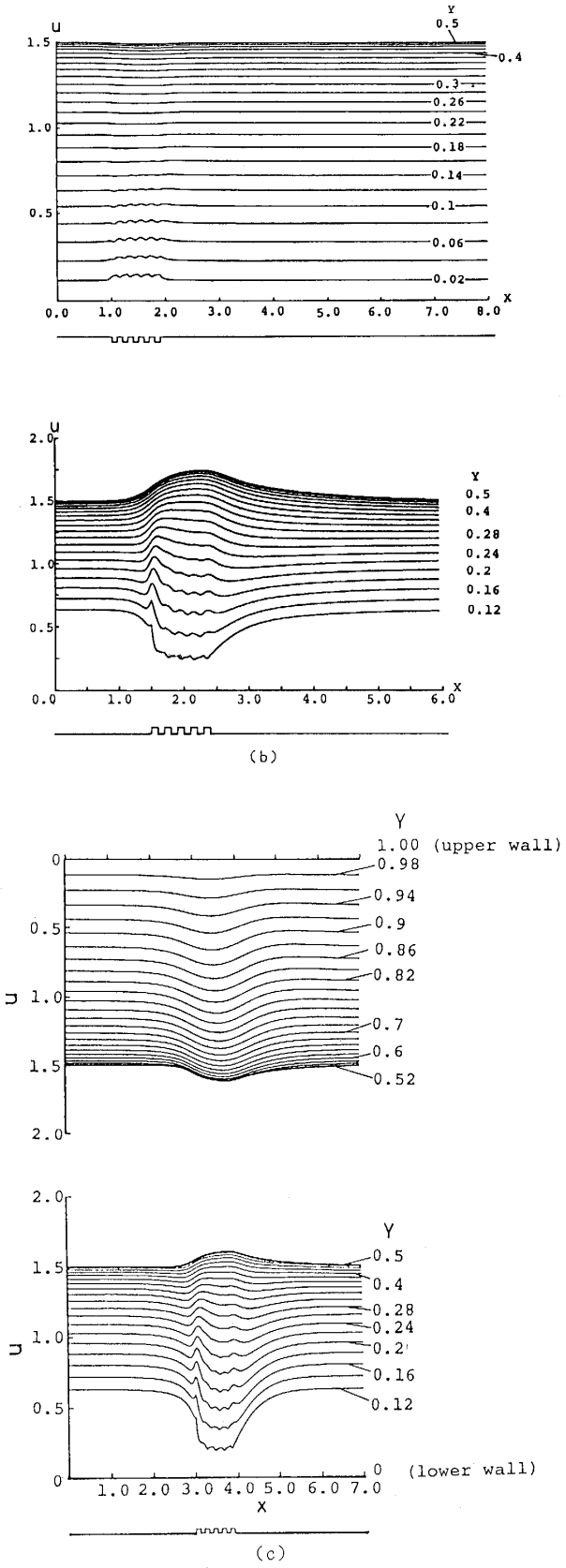

Fig. 4 Velocity distribution at the constant heights (Re=100), Flow is left to right; (a) Model I, (b) Model II, (c) Model III

increasing the distance to the downstream direction, while that of the central portion shows the contrary tendency. As can be seen in Fig.4(a) and (b), the tendency of velocity distribution for the case of model II is completely contrary to that of model I, that is, the velocity near the wall decreases at the region of rough wall compared with that of smooth wall, and more decreases in the region of rough surface as increasing the distance to the downstream direction. While that of the central portion increases considerably. In addition, the velocity near the rough wall increases suddenly at the portion just above the first roughness element. Considering from the phenomena of vortex pattern in the groove and of flow pattern over the rough wall decribed above, we note that the numerical results on the laminar flow are found to have similar quality compared with experimental results on the turbulent flow for the case of upstanding rough wall, by way of example as follow; the flow properties of turburent boundary layer are dominated by the effects of the first roughness element as being pointed out by Antonian and Luxton [26], and as presented by Sparrow et al. and the other [8~11], the highest heat transfer cofficient at the first roughness element of repeated square thermal ribs is resulted due to the effect of upstanding roughness on the flow in the rough wall channel. It can be seen in Fig.4(b) and (c) that the flow pattern near the rough wall for the case of model III have almost similar tendency for the case of model II. Here, we should note that the rough wall channel for the case of model III is the asymmetric geometry consisting of lower rough wall and upper smooth wall, so its flow pattern shows the asymmetric velocity distribution with respect to the center of channel, that is, the effect of lower rough wall on the flow reaches the opposite upper smooth wall of channel, and causes the velocity distribution to the decreasing velocity in lower region and the increasing velocity in upper region channel. This effect in such a case of model III is worth noting on the enhancement of heat transfer for the channel flow.

Fig.5 represents the distribution of difference velocity Δu obtained at the constant height, where Δu denotes the difference between u and u_r (the plane Poiseuille flow), for the cases of model I and II at $Re=100$. As can be seen in Fig.5(b), the streamwise distance of roughly 9 times the channel width (90 times the roughness height) is required to readjust from changed velocity with effect of roughness to the plane Poiseuille flow. The short readjustment distance for the case of embedded roughness compared with that of upstanding roughness is admitted (Fig.5(a)). It is also observed that the effect of roughness on the flow extends to the upstream region from rough surface for the both cases of embedded and upstanding roughness. However, from the comparison of both Δu distribution in Fig.5(a) and (b), the intense effect of upstanding roughness compared with that of embedded roughness is recognized.

In Fig.6, the relaxation distance X (the distance of readjustment to the plane Poiseuille flow) for the rough to smooth side is plotted against the Reynolds number for the model I, II and III. Fig.6 shows that the relaxation distance increases linealy with increasing the Renolds number, and depends on the geometry of rough surface.

Fig.7 shows the distribution of the normal velocity component v at the constant height. Here, the distribution of v for the embedded rough wall is shown for the case of $w/h=4$ calculated as an example, because the flow over the embedded roughness for $w/h=2$ skimmed along the roughness elements and groove (the existence of a

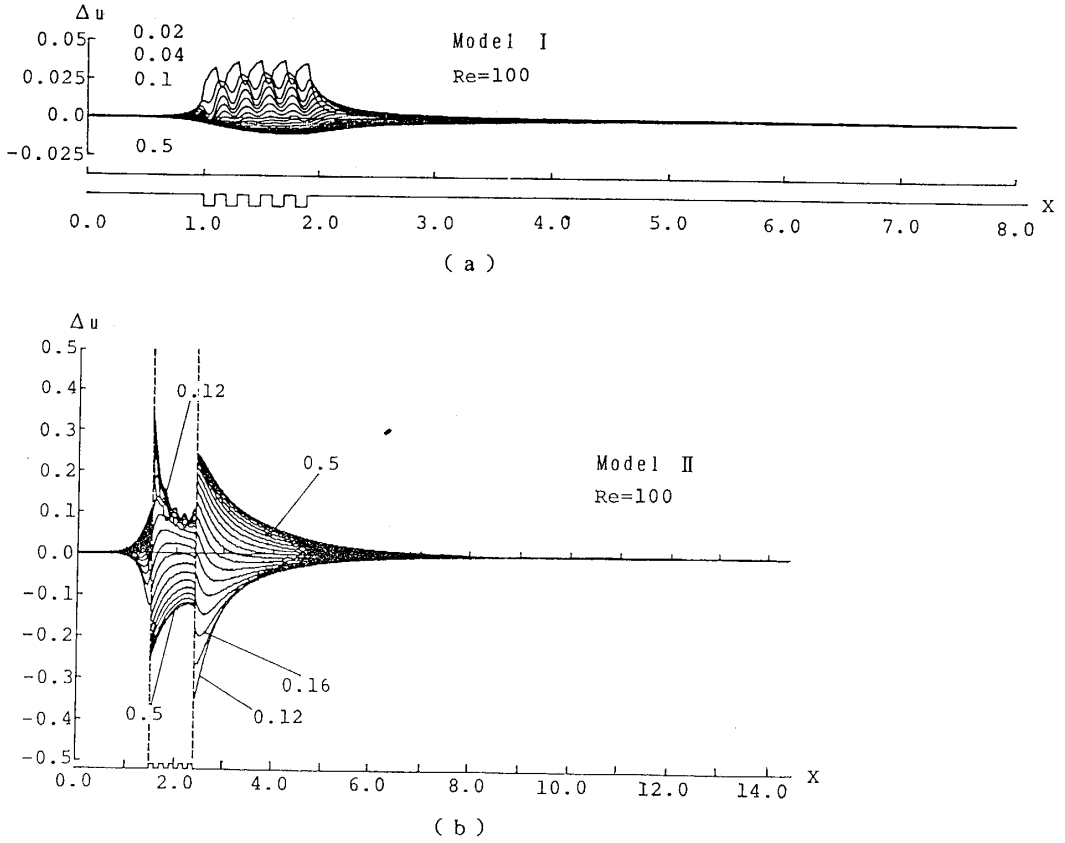

Fig. 5 Distribution of the velocity difference Δu
(a) Model I, (b) Model II.

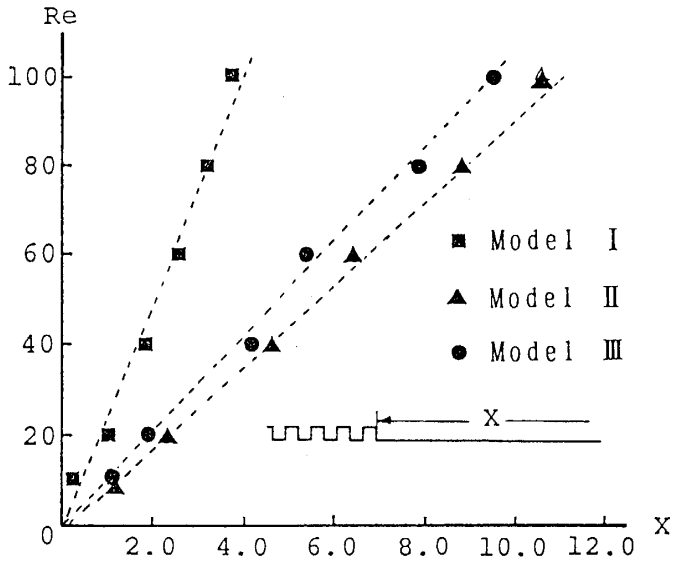

Fig. 6 Relation between the relaxation distance and the Reynolds number

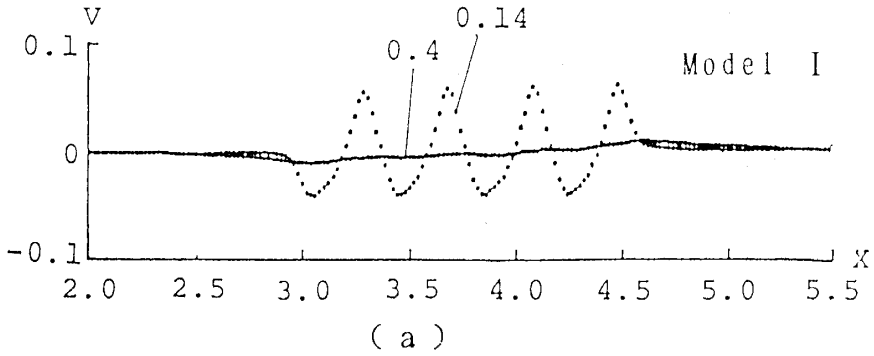

(a)

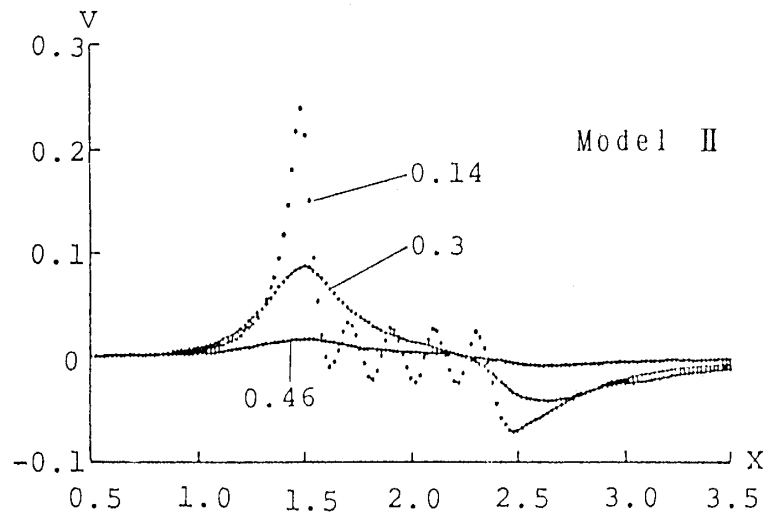

(b)

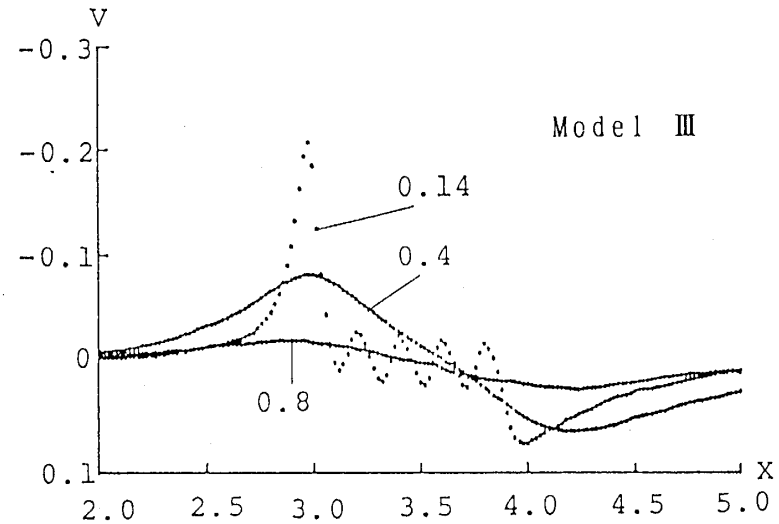

(c)

Fig. 7 Distribution of the normal velocity component v
(a) Model I (w/h=4), (b) Model II, (c) Model III

weak velocity v is recognized), while that of $w/h=4$ dipped into roughness groove [21, 25]. In Fig.7, the velocity v near the wall shows the periodic distribution in the similitude of roughness geometry for all cases, and its amplitude changes quite little at each location of successive roughness elements except the first element for upstanding roughness. The intense effect of first roughness element on velocity v is also for the upstanding roughness as shown in Fig.7(b) and (c). Noticeably, the v at the central region and even near the upper wall region is recognized for the case of upstanding rough wall.

From the results of flow pattern shown in Fig.3~7, it can be considered that the response of the channel flow to the roughness is quite different between the upstanding and embedded roughness, moreover, the adjustment process is also different between rough to smooth and smooth to rough sides.

3.2 *Distributions of pressure and wall shear stress*

In Fig.8(a)-(c), the pressure distributions along the channel at the constant height are shown for the Reynolds number $Re=100$ of each model I, II and III. The value of non-dimensional pressure P in Fig.8 is defined by the expression $P=Re\times(p'/\frac{1}{2}\rho U^2)$. Where p' denotes dimensional pressure, and express in the difference value from the base pressure level at the upstream boundary of channel. For all cases as shown in Fig. 8, the pressure distributions in the region of smooth wall show the constant value of non-dimensional pressure gradient to be equivalent to the plane Poiseuille flow ($-Re\times dp/dx=24$). In the region of rough wall, the pressure near the wall also shows the periodic pressure distribution in the similitude of the roughness geometry, and its periodic distribution becomes indistinct with increasing the distance from the wall and eventually disappears at the central region of channel. As can be seen in Fig.8(a) which is shown for the case of model I, the influence of embedded roughness on the pressure do not attain to the center line of channel. On the other hand, the effect of upstanding roughness on the pressure reaches the center line of channel as observed for the case of model II, and to the upper smooth wall of channel for the case of model III (Fig.8(b) and (c)). For the case of upstanding roughness, the effect of roughness on the pressure extends to the upstream region from rough surface, and its distance is equivalent to roughly 10 times the roughness height as can be seen in Fig.8(b) and (c). The value of non-dimensional pressure loss ΔP for the upstanding rough wall channel shows the large quantity as compared with that of embedded rough wall channel (as can be seen in Fig.8(a)), the value of ΔP for the embedded rough wall channel is approximately zero, in additon, the value of ΔP for model II is larger quantity than that of model III. In Fig.9, the pressure loss ΔP is plotted against the Reynolds number. Fig.9 shows that the ΔP for embedded rough wall is independent of the Reynolds number, and that of upstanding rough wall slightly decreases with increasing the Reynolds number.

In Fig.10(a)~(c), the distributions of wall shear stress are shown for the case of model I at $Re=400$ and of model II and III at $Re=100$. The wall shear stress is evaluated by the following equations which define the local skin friction coefficient:

$C_f=\tau'_w/(\frac{1}{2}\rho U^2)$ at the wall,

$C_f=\tau'_{xy}/(\frac{1}{2}\rho U^2)$ on the portion above the groove,

where $\tau'_w=\mu(\partial u'/\partial y')$ at wall and $\tau'_w=\mu(\partial v'/\partial x'+\partial u'/\partial y')_{y=0}$ (at $y=0.1$, provided it

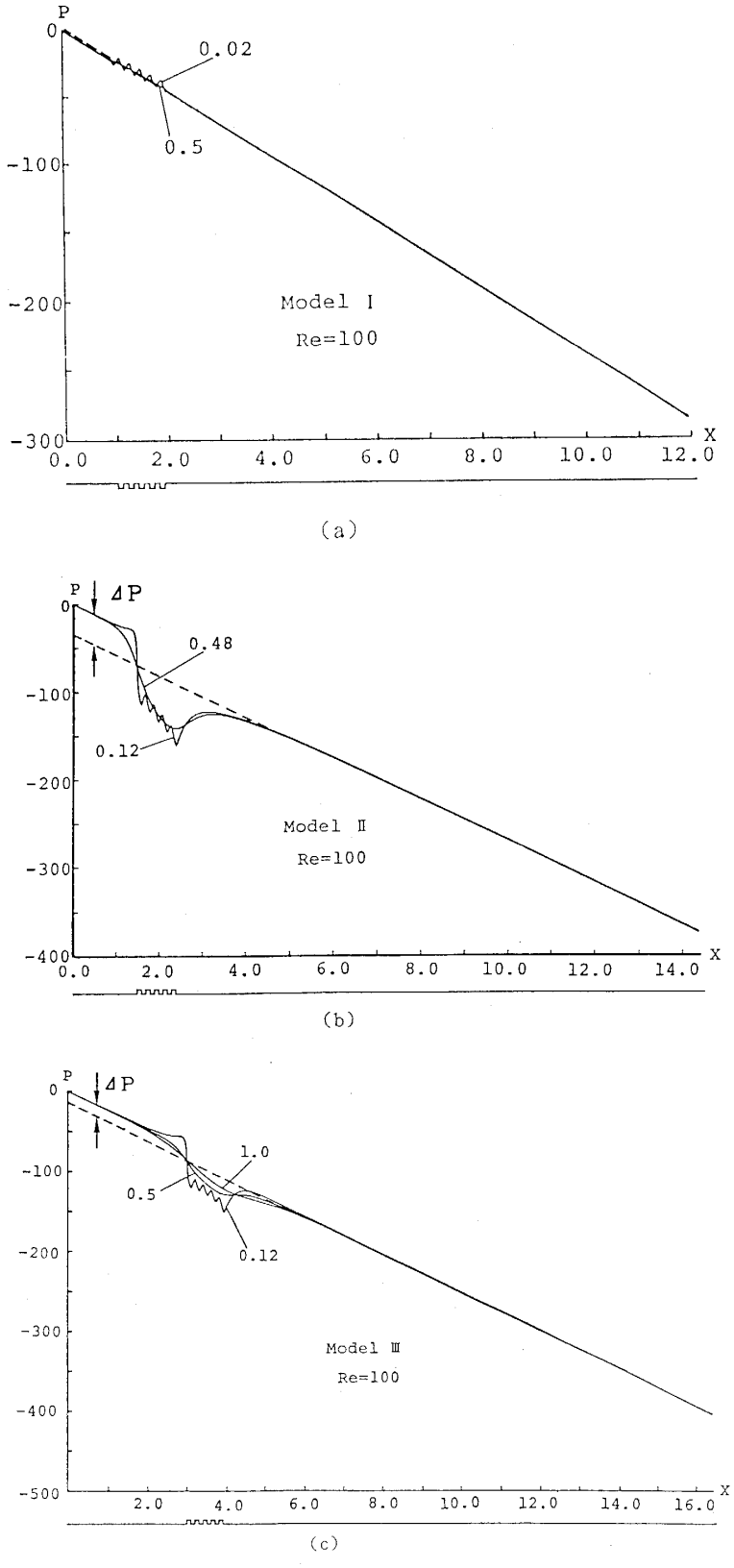

Fig. 8 Pressure distribution along the channel (Re=100);
(a) Model I (y=0.02, 0.5), (b) Model II (y=0.12, 0.5),
(c) Model III (y=0.12, 0.5, 1.0)

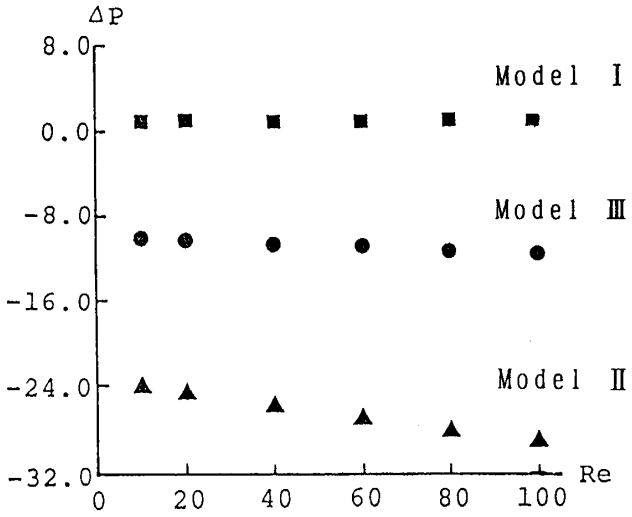

Fig. 9 Relation between the pressure loss and the Reynolds number

is the case of model II and III). Here, the notations with primes represent dimensional quantities.

As shown in Fig.10, the wall shear stress on the rough wall region varies periodically in similitude of roughness geometry, and its variation shows the high shear stress at the top of ribs and low shear stress at the portion of roughness groove (to be caused by the removal from restraint of wall). In the region of rough wall, the wall shear stress for the case of embedded rough wall (Fig.10(a)) gradually increases with increasing distance to the downstream direction, on the other hand, that of upstanding rough wall (Fig.10(b) and (c)) decreases with its distance. In addition, the shear stress at the first roughness element for the upstanding rough wall shows the highest quantity compared with that of the following downstream roughness elements. For the case of model III, the effect of rough wall (lower channel wall) on the flow reaches the opposite upper smooth wall of channel, for that reason, the increasing wall shear stress is also observed at its region (Fig.10(c)). It can be considered that such effects of increasing wall shear stress at smooth wall is worth noting on the application of enhancement of heat transfer. These tendencies for the wall shear stress correspond to the tendency of velocity distribution over the rough wall, vortex behavior in the groove and pressure distribution described above. Furthermore, it is interested that the wall shear stress for the upstanding rough wall is also considerably large compared with that of embedded rough wall in the same tendency as examined on the pressure loss. Thus, it can be understood and infered that both the total drag (frictional drag and pressure drag) and the heat transfer of upstanding rough wall channel are larger quantity than that of the embedded rough wall channel.

4. Conclusions

From the results and discussions described above, the following conclusions are summarized;

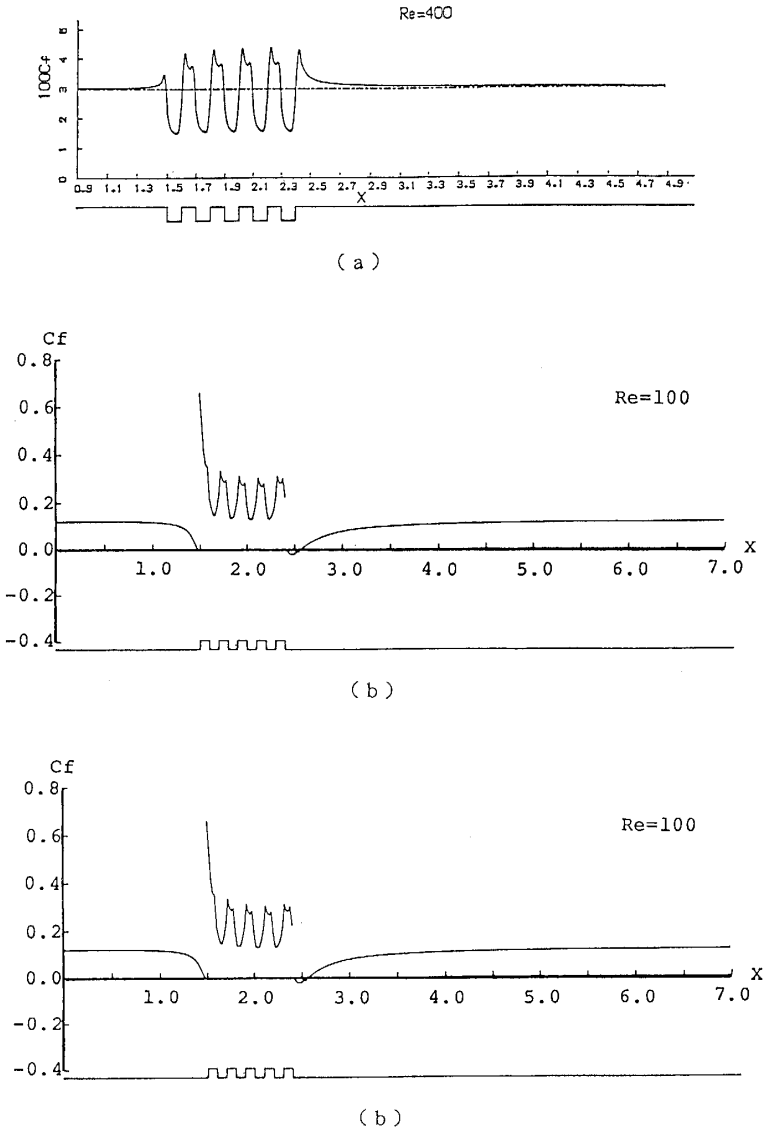

Fig.10 Distribution of wall shear stress, Flow is left to right;
(a) Model I, Re=400, (b) Model II, Re=100, (c) Model III, Re=100

(1) The stable separation vortex is formed in the roughness groove. For the case of embedded rough wall, this vortex develops gradually as the location of roughness groove being further downstream. In contrast with this tendency, that of upstanding rough wall shows the decreasing tendency.

(2) For the case of embedded rough wall, the velocity near the wall in the region of rough surface gradually increases with increasing the distance to the downstream direction, while that of the central region shows contrary tendency, and tendency of velocity distribution for the case of upstanding rough wall is completely contrary to that of embedded rough wall. In addition, the strong increase in velocity arises at the portion of first roughness element, and the existence of normal velocity component at the central region is recognized for the upstanding rough wall channel.

(3) The pressure loss ΔP for the upstanding rough wall channel shows large quantity as compared with that of embedded rough wall channel, that is, the pressure drag of

upstanding rough wall channel is larger than that of embedded rough wall channel. The pressure ΔP for embedded rough wall is independent of the Reynolds number, and that of upstanding rough wall slightly decreases with increasing the Reynolds number.
(4) The distribution of wall shear stress corresponds to the tendency of flow pattern, that is, tha wall shear stress for the case of embedded rough wall gradually increases with increasing the distance to the downstream direction, on the other hand, that of upstanding rough wall decreases with its distance. In addition, the shear stress at first roughness element for the upstanding rough wall shows the highest quantity compared with that of the following downstream roughness elements.
(5) For the case of model III (the channel consists of upper wall being smooth and lower wall being upstanding rough surface), the effect of lower rough wall on the flow reaches the opposite upper smooth wall of channel. So the shear stress and the pressure at the upper smooth wall and the velocity near the upper wall are affected considerably.
(6) The effect of roughness on the flow extends to the upstream region form rough surface, and its distance is equivalent to roughly 10 times the roughness height for the case of upstanding roughness at $Re=100$. The relaxation distance X for the rough to smooth side increases linearly with increasing the Reynolds number, and depends on the geometry of rough surface.

Acknowledgement

The authors would like to acknowledge the helpful suggestions and encouragements of Professor I.Nakamura of Nagoya University.

Reference

1) Schlighting,H.: Boundary Layer Theory, 7th ed., (1979), 616 McGrow-Hill.
2) Smits,A.J. and Wood,D.H.: The Response of Turbulent Boundary Layers to Sudden Perturbations, Ann. Rev. Fluid Mech., 17(1985), 321
3) Andreopoulos,J. and Wood,D.H.: The Response of Turbulent Boundary Layer to a Short Length of Surface Roughness, J. Fluid Mech., 118(1982), 143
4) Schofield,W.H.:Turbulent Shear Flows over a Step Change in Surface Roughness, Trans. ASME. 103, (1981), 344.
5) Nakayama,T.: Cooling of Electronic Divices, J. JSME, 88-802(1985), 48, (in Japanese)
6) Yanagida,T. and Kawasaki.: Pressure Drop and Heart Transfer Characteristics of Axial Air Flow through an Annulus with a Deep-Slotted Outer Cylinder and a Rotating Inner Cylinder, Trans. JSME, Ser. B, 53-493(1987), 2714, (in Japanese)
7) Yanagida,T.: A Caluculation Method for temperature Distribution of IC Packages on a Printed Wireing Bord, Trans. JSME, Ser, B. 54-503(1988), 1730, (in Japanese)
8) Sparrow,E.M., Vemuri,S.B. and Kadle,D.S.: Enhanced and Local Heat Transfer. Pressure Drop, and Flow Visualization for Array of Block-Like Electronic Components, Int. J. Heat Mass Transfer, 26-5(1983), 689
9) Sparrow,E.M., Niethhammer,J.E. and Chaboki,E.: Heat Transfer and Pressure Characteristics of Arrays Rectangular Modules Encountered in Microelectronic Equipment, Int. J. Heat Mass Transfer, 25-7(1982), 961
10) Moffat,R.J., Arvizu,D.E. and Ortega, A.: Cooling Electronic Components. Forced Convection

Experiments with an Air-Cooled Arrays, Heat Transfer in Electronic Equipment. HTD, 48(1985) 17

11) Hoi,Y.M. and Park,K.A.: Forced Convective Heat Transfer in a Channel with Arrays of Similated Microelectronic Chips. Proc. 1st KSME-JSME Thermal Fluids Eng., 2(1988), 371
12) Savides,C.N. and Gerrrard,J.H.: Numerical Analysis of the Flow through a Corrugated Tube with Application to Arterial Prostheses, J. Fluid Mech., 138(1984), 129
13) Sobey,I.J.: On Flow through Narrowed Channels. Part 1. Calculated Flow Patterns, J. Fluid Mech., 96(1986), 1
14) Sobey,I.J.: The Occurrence of Separation in Oscillatory Flow. J. Fluid Mech., 134(1980), 247
15) Nishimura,T., Ohori,Y. and Kawamura,Y.: Flow Characteristic in a Channel with Symmetric Wavy Wall for Stedy Flow. J. Chem. Eng. Japan, 17-5(1984), 466
16) Nishimura,T., Ohori,Y., Kajimoto,Y. and Kawamura,Y.: Mass Transfer Characteristic in a Channel with Symmertic Wavy Wall for Steady Flow. J. Chem. Eng. Japan, 18-6(1985), 550
17) Nishimura,T., Kajimoto,Y. and Kawamura,Y.: Mass Transfer Enhancement in Channels with a Wavy Wall. J. Chem. Eng. Japan, 19-2(1985), 142
18) Nishimura,T., Kajimoto,Y., Tarumoto,A. and Kawamura,Y.: Flow Structure and Mass Transfer a Wavy Channel in Transitional Flow Regime. J. Chem. Eng. Japan, 19-5(1986),449
19) Nakanishi,S. and Osaka,H.: A Numerical Study on the Blood Flow in an Artery with a Rough Surface, 1st Report, Steady Flow. Trans. JSME, Ser. B, 52-484(1986), 3931, (in Japanese)
20) Nakanishi,S. and Osaka,H.: A Numerical Study on the Blood Flow in an Artery with a Rough Surface, 2nd Report, Pulsatile Flow. Trans. JSME. Ser. B, 52-484(1986), 3935, (in Japanese)
21) Nakanishi,S. and Osaka.H.: Flow through a Channel with Two-Dimensional Repeated Square Ribs, 1st Report, Classification of the Flow Pattern, Trans. JSME, Ser. B, 55-516(1989), 2181. (in Japanese)
22) Nakanishi,S. and Osaka,H.: Flow through a Channel with Two-Dimensional Repeated Square Ribs, 2nd Report. Dynamical Characteristics, Trans.JSME, Ser. B, 55-516(1989), 2191. (in Japanese)
23) Nakanishi,S. and Osaka,H.: Flow Pattern in a Two-Dimensional Rough Wall Channel, Proc. 1st KSME-JSME Thermal Fluids Eng., 2(1988), 26
24) Nakanishi,S. and Osaka,H.: Structure of the Pulsatile Blood Flow in the Vascular with a Rough Wall. Tech. Rep. Yamaguchi Univ., 4-2(1988), 95
25) Nakanishi,S. and Osaka.H.: Structure of the Blood Flow in the Vascular with a Rough Wall, Memories of Faculty of Eng. Yamaguchi Univ. 4-2(1988), 95, (in Japanese)
26) Antonia.R.A. and Luxton,R.E.: The Response of a Truburent Boundary Layer to an Upstanding Step Change in Surface Roughness, Trans. ASME, Ser. D, 98(1971), 22